Supplementary material for

Archaeological mitogenomes illuminate the historical ecology of sea otters (*Enhydra lutris*) and the viability of reintroduction

Hannah P. Wellman, Rita M. Austin, Nihan D. Dagtas, Madonna L. Moss, Torben C. Rick, Courtney A. Hofman

Contents:

Supplementary Material Text

Supplementary Material Figures S1-S10

Supplementary Material Table S1: Detailed specimen metadata
Wellmanetal_TableS1.xlsx

Supplementary Material Table S2: DNA Pipeline Summary/Statistics
Wellmanetal_TableS2.xlsx

Supplementary Material Table S3: Haplotypes summary
Wellmanetal_TableS3.xlsx

Supplementary Material Text

Archaeological Materials

The Par-Tee (35CLT20) and Palmrose (35CLT47) sites are coastal shell middens excavated between 1967 and 1977 at Seaside, Oregon (1), located about 28km south of the mouth of the Columbia River. Par-Tee is located closest to the shoreline and dates to 1850-1150 B.P. (calendar years before present; (2)), while Palmrose (2600-1600 calendar years B.P.; (3,4)) is located ~1 mile inland. The sites were excavated by Robert Drucker and George Phebus and their volunteers in 5 × 5 foot (~1.5 × 1.5 m) units in arbitrary one-foot (~30 cm) levels. All sediments were screened over 1/4-inch mesh (1). Unit depths varied, reaching up to six feet (1.8 m) in some locations. Phebus and Drucker sampled around 550m^2 at Par-Tee, making it one of the "most extensively excavated sites on the Northwest Coast south of Ozette" (5). The Par-Tee (35CLT20) assemblage is housed at the Smithsonian Institution National Museum of Natural History (NMNH) in Washington, D.C. The Palmrose (35CLT47) assemblage is split between the NMNH and the Museum of Natural and Cultural History (MNCH) at the University of Oregon in Eugene. We sampled twenty right lower first molars (M_1s): ten from Palmrose, and ten from Par-Tee, thus ensuring that each tooth represented a single individual. We chose right M_1s because they represented the total highest Minimum Number of Individuals (MNI=50) in the two sites, and were overall well preserved.

Historical Dental Calculus Samples

We used dental calculus (calcified plaque) from 21 historical Pacific Coast sea otters as a source for mitogenomes to compare to the archaeological Oregon sea otters. Although these samples range in age from ~1859 to 1983, and encompass pre-extirpation and post-fur trade eras, we consider them historical due to their age (>30 years old) and the fragmented preservation of endogenous DNA in calculus (6,7). Five of the specimens date from ~1859-1911, just prior to/concurrent with the fur trade extirpations (8,9), while eleven date to 1949 or later, representing post-fur trade populations. Four of the specimens were undated. Four specimens are reintroduction-era (1960s) Amchitka Island sea otters. Amchitka Island sea otters served as the source population for reintroductions to Southeast Alaska, British Columbia, and Washington, and therefore likely reflect present genetic diversity in those areas (8), precluding the need for additional sampling of modern northern individuals and serving as the northern comparison for this study. Sixteen of the skulls sampled for calculus are housed in the Department of Mammals at the NMNH, and five are in the collections of the Santa Barbara Museum of Natural History (SBMNH), California. Specimen metadata and photographs are in Table S1 and Figures S2-S3.

Previous Phenotype Studies

Roest (10) analyzed various morphological traits to determine phenotypic traits by subspecies. Wilson et al. (11) defined three subspecies: *E. l. lutris* from the Kuriles north to the Commander Islands, *E. l. kenyoni* from the Aleutians to Washington, and *E. l. nereis* for California and south. They found pre-reintroduction Oregon sea otters were intermediate to California and northern sub-populations, but more "properly classified" with Alaska sea otters (11). Lyman (12) and Wellman (13) used archaeological and modern crania, teeth, and long bones to investigate how Oregon sea otters compared phenotypically to modern California and Alaska sea otters. Lyman found archaeological Oregon sea otter teeth were intermediate in size between modern California and Alaska sea otters (12). Wellman replicated Lyman's study and expanded the tooth sample

size and incorporated humeri and femora measurements (13). Wellman concluded, similarly to Lyman and Wilson et al., that archaeological Oregon sea otter measurements were intermediate between modern California and Alaska sea otters, and that variation in size occurred on a latitudinal cline. Wellman found more Oregon measurements were significantly different from those from California, compared to Lyman who noted more overlap between Oregon and California. The slight differences in results between Wellman and Lyman are consistent with variation on a latitudinal cline: Wellman analyzed archaeological sea otter specimens from the Par-Tee and Palmrose sites located on the northern Oregon coast, while Lyman measured sea otters from the central/southern Oregon coast.

Genetic analysis

Ancient and Historical DNA Sampling

All ancient DNA labwork was performed in the Laboratories of Molecular Anthropology and Microbiome Research (LMAMR) at the University of Oklahoma, Norman. The Ancient DNA Laboratory at LMAMR follows established contamination control workflows (14,15), including physical separation from all laboratories in which PCR is performed, unidirectional work flows to avoid cross-contamination, regular sterilization of all work surfaces with bleach solution, overhead UV lights, and the use of full body Tyvek suits, masks, and gloves by all researchers.

The archaeological sea otter teeth were cleaned with a dilute bleach solution to remove surface contamination. A Dremel was used to abrade/remove remaining debris and the outermost layer of cementum from the tooth root being sampled. The root was then removed from the crown. The root was ground into a powder and ~100 mg was used for DNA extraction. In the research collections at NMNH and SBMNH, dental calculus was carefully removed from the tooth using a dental scaler directly into a sterile Eppendorf tube. Each tube is placed in a "bowl" shaped from tin foil, ensuring the dental calculus is contained and will not contaminate other tubes or the work surface. Gloves were changed between taking samples, cleaning, or handling specimens.

Ancient and Historical DNA Extraction

Ancient dentine and historical calculus samples were decontaminated in a UV Crosslinker and predigested in 1 ml of EDTA (0.5 M) for 15 minutes. The supernatant was removed and an additional 1 ml of EDTA (0.5 M) was added to the samples which were placed on a rotating nutator at room temperature overnight. 100 uL of Qiagen proteinase K was added to the samples which were returned to the rotating nutator at room temperature for two days. The dentine samples underwent a second round of EDTA and proteinase K treatment. DNA was extracted using a modified existing silica-extraction protocol (16,17).

High Throughput Sequencing Library Preparation

Library preparation on the ancient dentine and historical calculus samples was performed following previously published protocols (18). Up to 100 mg of DNA was treated with a half reaction of UDG to repair ancient DNA damage while maintaining the terminal damage required to verify molecule authenticity (19). UDG-half treated samples were built into dual indexed Illumina shotgun libraries using a NEBNext DNA Library for 454 Master Mix kit, then cleaned with silica column purification (Qiagen MinElute PCR Purification Kit). Library preparation on the historical samples was performed following the previously published BEST protocols (20) which also included partial UDG treatment (19) followed by SPRI bead purification. Ancient and

historical libraries were quantified using a qPCR SYBRGreen Assay to determine PCR cycle number. Both ancient and historical libraries were then amplified in triplicate between 10 and 24 cycles at the following PCR program: initial denaturation at 95 °C for 5 min, denaturation at 98 °C for 20 s, annealing at 60°C for 15 s, elongation at 72°C for 30 s, and a final elongation at 72°C for 1 min.

Mitogenome Capture

Following PCR amplification, ancient and historical samples were cleaned using SPRI bead purification and quantified using a fluorometer (Qubit). The ancient and historical mtDNA genomes were captured using custom *Enhydra lutris* bait probes (myBaits) following the myBaits protocol (MYBaits User Manual version 3.02). In brief, the cleaned libraries were allowed to hybridize with the baits in the thermal cycler at 60 °C for 48 hours. The captured libraries were then bound to Dynabeads MyOne Streptavidin C1 beads by hybridizing in the thermal cycler for three 3 min cycles at 60 °C. Following purification according to the myBaits protocol, the captured libraries were assayed using qPCR and amplified as follows: initial denaturation at 98 °C for 2 min, 12-22 cycles of denaturation at 98 °C for 20 s, annealing at 60°C for 15 s, elongation at 72°C for 30 s, and a final elongation at 72°C for 5 min. The captured, amplified libraries were removed from the beads and pooled. The libraries were then analyzed for fragment length using Fragment Analyzer, pooled in equimolar ratios and adapter dimers were removed by selecting fragments within 150 bp to 500 bp size range on the PippinPrep. The pooled libraries were sequenced on an Illumina MiSeq 2 x 150 at the University of Oklahoma Consolidated Core Laboratory.

Bioinformatic analyses

After capture, reads were processed using a pipeline tailored to ancient mitogenomic analysis. Paired reads were merged, trimmed, and adapter sequences removed with Adapter Removal2 (v. 2.1.7); (21). Reads were mapped to a reference sea otter mitogenome (22) using Burrows Wheeler Aligner (bwa v. 0.7.17); (23) with minor modifications (-l 1000 –n 0.1). Reads were filtered and sorted to remove duplicates, low quality, and unmapped reads (samtools) (24). BAM files were processed with MapDamage2 (25) to evaluate ancient DNA damage patterns and authenticity using fragment length plots (Figs. S4 and S5). Qualimap2 was used to generate genome coverage statistics. Variant calls were made using samtools mpileup and VarScan2 (v. 2.4.3) on rescaled BAM files. Unusual numbers of heterozygous SNP calls were generated in the sequences derived from dental calculus. After ruling out possible contamination by mapping sequences to the human mitogenome, the mapping parameters were modified to those specified above, and variant calls in the rescaled bam files were examined manually in Geneious (v. 11.1.4).

The rescaled bam files were rendered into consensus sequences in Geneious and aligned with MAFFT as implemented in Geneious (26,27). The alignment was visually inspected. Positions 2655/2656 appear to be the result of deletion or amplification errors. These positions were manually edited to N as a conservative call prior to downstream analysis. Additional positions 16,375-16,432 in D-loop were removed for downstream analysis due to missing data and poor alignment. Four historical samples (188634, A49492, 1366F, 285441) failed quality control and two archaeological samples (PRSE2G-3, PRNE1K-3) were not sequenced successfully and were excluded from downstream analysis.

PopArt was used to estimate a median-joining network (28,29). Haplotype diversity was calculated in DnaSP (v. 6) (30). In order to explore and visualize the temporal signal associated with haplotype diversity, we used TempNet in R (v. 3.6.3). The alignment was separated by rough time period (Palmrose and Par-Tee sites, respectively, and historical). Alignments were stripped for identical sites and ambiguities in Geneious prior to TempNet analysis. Raw sequence data are available through the NCBI Short Read Archive (SRA) under BioProject accession PRJNA550086. Consensus sequences and the alignment used for analysis (ModAlign.fa) are available from the Dryad Digital Repository (https://doi.org/10.5061/dryad.djh9w0vxz).

Phylogenetic Analysis

Given the well-dated contexts and specimens we attempted to estimate tMRCA for populations in this study using BEAST. One sample from each haplotype was aligned as described above. To evaluate the temporal signal in the data and identify outlier samples, we generated a neighbor joining tree with Geneious Tree Builder with the Jukes-Cantor model and 1000 bootstrap replicates for use with TempEst (v. 1.5.3) (Fig. S6).

For each sample a tip date was provided to TempEst. Archaeological sample dates (PR and PT in figure) were based on published AMS radiocarbon dates (Palmrose: 2600-1600 BP (3,4) and Par-Tee: 2300-800 BP (2)). Historical samples were given collection dates associated with the specimens. If collection date was unknown 1900 ± 100 was used. The modern California samples were collected between 2000 and 2014 (31), so 2007 ± 7 was used. The heuristic residual mean squared analysis with best-fitting root indicated poor temporal signal (R squared 0.1215). The estimated time tMRCA for all samples in this analysis was 15,993 years BP. One sample in particular (188636) from the Kurile Islands of Japan is less divergent than sampling age (blue) while several others are more divergent than their sampling age (red) (Fig. S7). We repeated the analysis without sample 188636 and the R squared remained low (0.1568) (Fig. S8).

Additionally, we evaluated both codon and gene partitions (excluding tRNAs) using PartitionFinder (v. 2.1.1) and identified three partitions using the AIC criteria. The first partition consisted of 16S, 12S, and the first codon site for each gene, except ND5 in which it was the second codon site. The second partition included the second codon site for all genes but the third codon site for ND5 and the last partition consisted of the third codon site and the first codon for ND5. ND5 is transcribed in the opposite direction of the other genes. We used these partitions to conduct maximum likelihood phylogenetic analysis with IQ-TREE (32) as implemented on IQ-TREE (v. 1.6.12) with 1000 bootstrap replicates (Fig. S9). IQ-TREE selected the HKY+F+I model for partition one and HKY+F for partitions two and three. When analyzed in TempEst, this phylogeny (Fig. S10) yielded similar, poor temporal results (low R squared value = 9.3485E-2). The consistent low R squared values across these analyses suggest it is not suitable to pursue a tip dated phylogenetic analysis.

Prior Genetic Studies

Previous genetic analyses suggested that archaeological Oregon sea otters shared haplotypes with California sea otters (33,34). To establish whether these patterns held when combined with the data sequenced for this study the Larson et al. and Valentine et al. sequences were aligned to the final alignment which was trimmed to account for the minimum length of the previously published sequences (222 bp). A median-joining network was created in PopArt (28,29). The resulting network (Figure S1) differs from the network generated with complete mitogenomes

(Figure 2): the archaeological Oregon sea otters are split and assigned to single modern California (blue) and Alaska (green) haplotypes, the historical Washington and B.C. samples are grouped with the California haplotype, and the clear division between California and northern haplotypes is eliminated. Trimming the alignment excluded base changes present in the complete mitogenome outside of the 222 bp D-loop section. The difference in interpretation suggests that complete mitogenome analyses, now enabled by reduced costs and advances in Next Generation Sequencing (NGS), may better capture overall diversity in haplotypes than smaller sequences.

References

1. Phebus GE, Drucker RM. Archaeological Investigations in Seaside, Oregon: An Intermediate Report on the Excavations of Two Major Archaeological Sites at Seaside, Oregon, Through September, 1977. Seaside, Oregon: Seaside Museum and Historical Society; 1979.

2. Sanchez GM, Rick TC, Culleton BJ, Kennett DJ, Buckley M, Erlandson JM, et al. Radiocarbon dating legacy collections: A Bayesian analysis of high-precision AMS 14C dates from the Par-Tee site, Oregon. Journal of Archaeological Science: Reports. 2018 Oct;21:833–48.

3. Connolly TJ. Archaeological Evidence for a Former Bay at Seaside, Oregon. Quaternary Research. 1995;43:362–9.

4. Connolly TJ. Human responses to change in coastal geomorphology and fauna on the southern Northwest coast: Archaeological investigations at Seaside, Oregon. University of Oregon; 1992. (University of Oregon Anthropological Papers).

5. Losey RJ, Yang DY. Opportunistic Whale Hunting on the Southern Northwest Coast: Ancient DNA, Artifact, and Ethnographic Evidence. Am antiq. 2007 Oct;72(4):657–76.

6. Mann AE, Sabin S, Ziesemer K, Vågene ÅJ, Schroeder H, Ozga AT, et al. Differential preservation of endogenous human and microbial DNA in dental calculus and dentin. Sci Rep. 2018 Dec;8(1):9822.

7. Austin RM, Sholts SB, Williams L, Kistler L, Hofman CA. Opinion: To curate the molecular past, museums need a carefully considered set of best practices. Proc Natl Acad Sci USA. 2019 Jan 29;116(5):1471–4.

8. Kenyon KW. The Sea Otter in the Eastern Pacific Ocean. New York: Dover Publications; 1969.

9. Scheffer VB. The Sea Otter on the Washington Coast. The Pacific Northwest Quarterly. 1940;31(4):370–88.

10. Roest AI. Subspecies of the Sea Otter, Enhydra lutris. Contributions in Science. 1973;(252):1–17.

11. Wilson DE, Bogan MA, Brownell RL, Burdin AM, Maminov MK. Geographic Variation in Sea Otters, Enhydra lutris. Journal of Mammalogy. 1991 Feb 13;72(1):22–36.

12. Lyman R. Zoogeography of Oregon Coast Marine Mammals: The Last 3,000 Years. Marine Mammal Sci. 1988 Jul;4(3):247–64.

13. Wellman HP. Applied zooarchaeology and Oregon Coast sea otters (*Enhydra lutris*). Marine Mammal Science. 2018 Jul;34(3):806–22.

14. Yang DY, Watt K. Contamination controls when preparing archaeological remains for ancient DNA analysis. Journal of Archaeological Science. 2005 Mar;32(3):331–6.

15. Shapiro B, Hofreiter M, editors. Ancient DNA [Internet]. Totowa, NJ: Humana Press; 2012 [cited 2020 Sep 8]. (Methods in Molecular Biology; vol. 840). Available from: http://link.springer.com/10.1007/978-1-61779-516-9

16. Dabney J, Knapp M, Glocke I, Gansauge M-T, Weihmann A, Nickel B, et al. Complete mitochondrial genome sequence of a Middle Pleistocene cave bear reconstructed from ultrashort DNA fragments. Proceedings of the National Academy of Sciences. 2013 Sep 24;110(39):15758–63.

17. Morales-Arce AY, Hofman CA, Duggan AT, Benfer AK, Katzenberg MA, McCafferty G, et al. Successful reconstruction of whole mitochondrial genomes from ancient Central America and Mexico. Sci Rep. 2017 Dec;7(1):18100.

18. Meyer M, Kircher M. Illumina Sequencing Library Preparation for Highly Multiplexed Target Capture and Sequencing. Cold Spring Harb Protoc. 2010 Jun 1;2010(6):pdb.prot5448.

19. Rohland N, Harney E, Mallick S, Nordenfelt S, Reich D. Partial uracil–DNA–glycosylase treatment for screening of ancient DNA. Phil Trans R Soc B. 2015 Jan 19;370(1660):20130624.

20. Carøe C, Gopalakrishnan S, Vinner L, Mak SST, Sinding MHS, Samaniego JA, et al. Single-tube library preparation for degraded DNA. Methods in Ecology and Evolution. 2018;9(2):410–9.

21. Schubert M, Lindgreen S, Orlando L. AdapterRemoval v2: rapid adapter trimming, identification, and read merging. BMC Research Notes. 2016;9:88.

22. Yonezawa T, Nikaido M, Kohno N, Fukumoto Y, Okada N, Hasegawa M. Molecular phylogenetic study on the origin and evolution of Mustelidae. Gene. 2007 Jul;396(1):1–12.

23. Li H, Durbin R. Fast and accurate long-read alignment with Burrows-Wheeler transform. Bioinformatics. 2010 Mar 1;26(5):589–95.

24. Li H, Handsaker B, Wysoker A, Fennell T, Ruan J, Homer N, et al. The Sequence Alignment/Map format and SAMtools. Bioinformatics. 2009 Aug 15;25(16):2078–9.

25. Ginolhac A. mapDamage: testing for damage patterns in ancient DNA sequences. Bioinformatics. 2011;27:2153–5.

26. Katoh K. MAFFT: a novel method for rapid multiple sequence alignment based on fast Fourier transform. Nucleic Acids Research. 2002 Jul 15;30(14):3059–66.

27. Katoh K, Standley DM. MAFFT Multiple Sequence Alignment Software Version 7: Improvements in Performance and Usability. Molecular Biology and Evolution. 2013 Apr 1;30(4):772–80.

28. Bandelt HJ, Forster P, Rohl A. Median-joining networks for inferring intraspecific phylogenies. Molecular Biology and Evolution. 1999 Jan 1;16(1):37–48.

29. Leigh JW, Bryant D. popart: full-feature software for haplotype network construction. Methods in Ecology and Evolution. 2015;6(9):1110–6.

30. Rozas J, Ferrer-Mata A, Sánchez-DelBarrio JC, Guirao-Rico S, Librado P, Ramos-Onsins SE, et al. DnaSP 6: DNA Sequence Polymorphism Analysis of Large Data Sets. Molecular Biology and Evolution. 2017 Dec 1;34(12):3299–302.

31. Ralls K, McInerney NR, Gagne RB, Ernest HB, Tinker MT, Fujii J, et al. Mitogenomes and relatedness do not predict frequency of tool-use by sea otters. Biol Lett. 2017 Mar;13(3).

32. Trifinopoulos J, Nguyen L-T, von Haeseler A, Minh BQ. W-IQ-TREE: a fast online phylogenetic tool for maximum likelihood analysis. Nucleic Acids Res. 2016 Jul 8;44(W1):W232–5.

33. Valentine K, Duffield DA, Patrick LE, Hatch DR, Butler VL, Hall RL, et al. Ancient DNA reveals genotypic relationships among Oregon populations of the sea otter (Enhydra lutris). Conserv Genet. 2008 Aug;9(4):933–8.

34. Larson S, Jameson R, Bodkin J, Staedler M, Bentzen P. Microsatellite DNA and Mitochondrial DNA Variation in Remnant and Translocated Sea Otter (Enhydra lutris) Populations. Journal of Mammalogy. 2002;83(3):893–906.

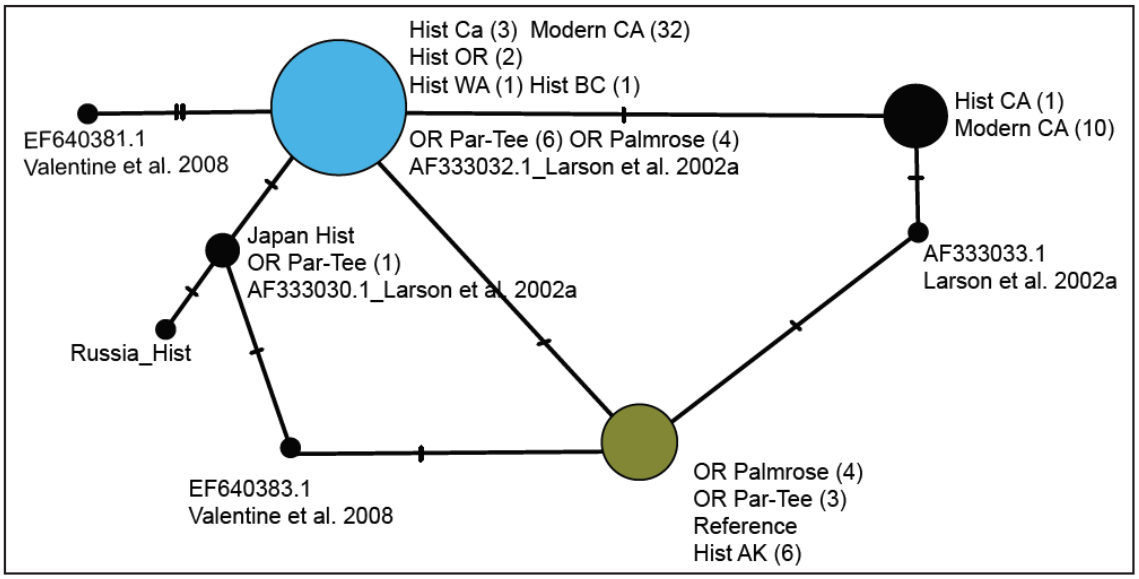

Fig. S1. Median joining network of trimmed alignment including Larson et al. 2002a and Valentine et al. 2008 data. Nodes represent unique haplotypes; node size represents haplotype frequency. Hash marks represent nucleotide changes between haplotypes.


Fig. 2A: Archaeological specimen PTSE7F-6

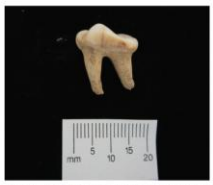
Fig. 2B: Archaeological specimen PTSE8J-8


Fig. 2G: Archaeological specimen PTSE5J-8


Fig. 2H: Archaeological specimen PTSALV

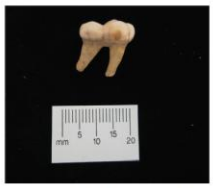
Fig. 2C: Archaeological specimen PTSE14J-7

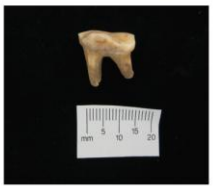
Fig. 2D: Archaeological specimen PTSE5G-7


Fig. 2I: Archaeological specimen PTSE11J-8


Fig. 2J: Archaeological specimen PTSE13K-4

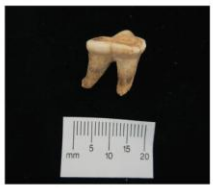
Fig. 2E: Archaeological specimen PTSW19H-8

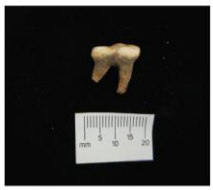
Fig. 2F: Archaeological specimen PTNE12G-9


Fig. 2K: Archaeological specimen PRSW6N-3

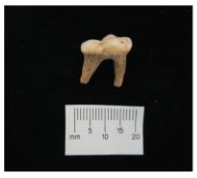
Fig. 2L: Archaeological specimen PRSW5D-4

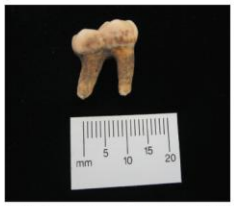
Fig. 2M: Archaeological specimen PRNE1E-5


Fig. 2N: Archaeological specimen PRNE1G-3

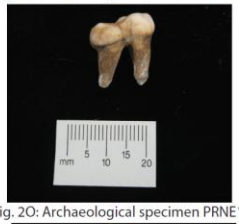
Fig. 2O: Archaeological specimen PRNE1I-5


Fig. 2P: Archaeological specimen PRNE1K-3

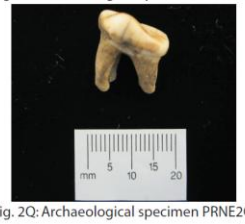
Fig. 2Q: Archaeological specimen PRNE2Q-6


Fig. 2R: Archaeological specimen PRNE4E-4


Fig. 2S: Archaeological specimen PRSE2G-3

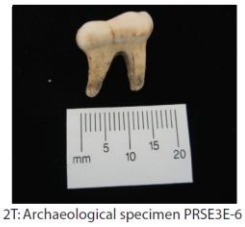
Fig. 2T: Archaeological specimen PRSE3E-6

Fig. S2. Photos of archaeological specimens prior to sampling. Palmrose specimens are labeled "PR" and Par-Tee specimens are labeled "PT," followed by their provenience.

Fig.3A: NMNH sea otter specimen 285470

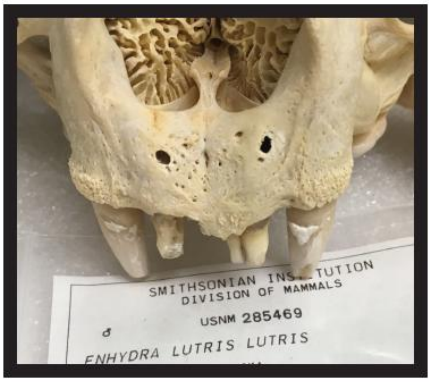

Fig. 3B: NMNH sea otter specimen 285469

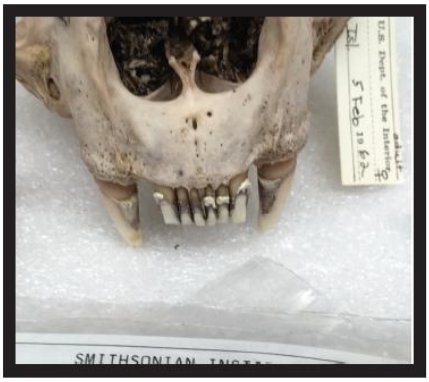

Fig. 3C: NMNH sea otter specimen 527170

Fig. 3D: NMNH sea otter specimen 527162

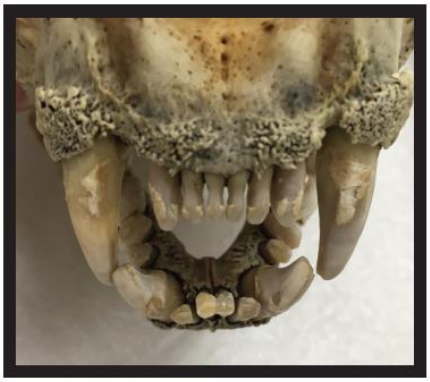

Fig. 3E: NMNH sea otter specimen 396641

Fig. S3. Photos of selected historical dental calculus specimens prior to sampling.

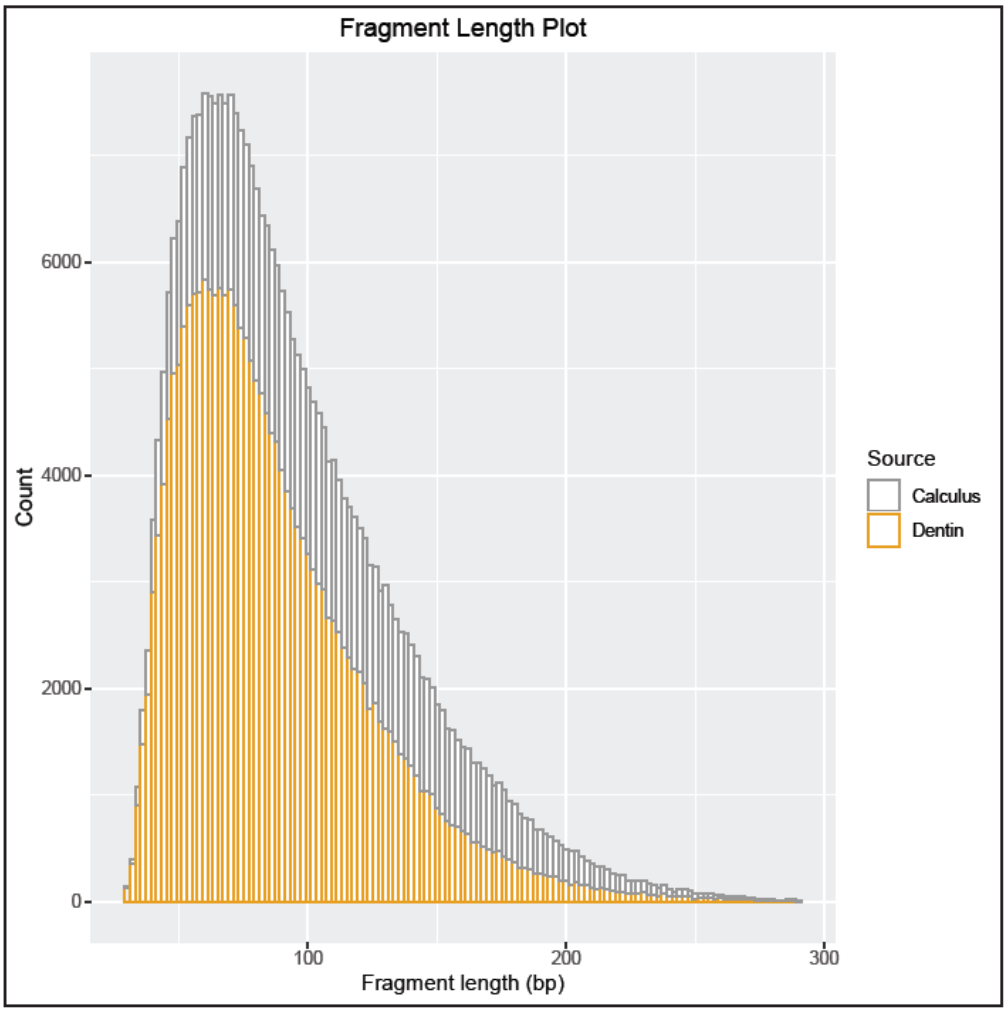

Fig. S4. Fragment length plot for ancient dentine (yellow) and historical calculus (gray) samples.

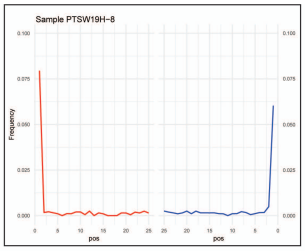

Fig. 5A: Sample PTSW19H-8, 19095 Q37 mapped reads.

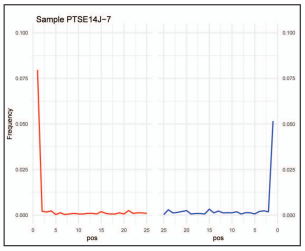

Fig. 5D: Sample PTSE14J-7, 45766 Q37 mapped reads.

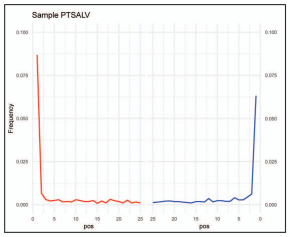

Fig. 5G: Sample PTSALV, 75197 Q37 mapped reads.

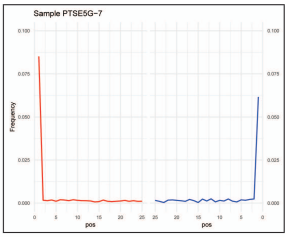

Fig. 5J: Sample PTSE5G-7, 249319 Q37 mapped reads.

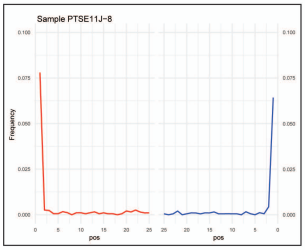

Fig. 5B: Sample PTSE11J-8, 17255 Q37 mapped reads.

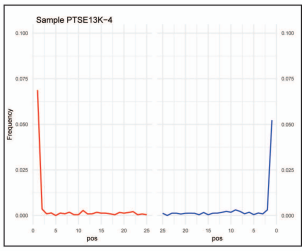

Fig. 5E: Sample PTSE13K-4, 44417 Q37 mapped reads.

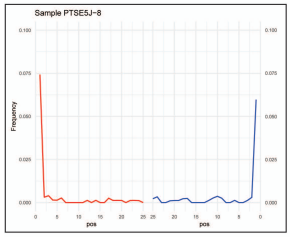

Fig. 5H: Sample PTSE5J-8, 6001 Q37 mapped reads.

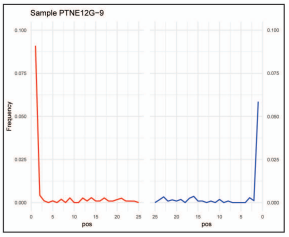

Fig. 5K: Sample PTNE12G-9, 8257 Q37 mapped reads.

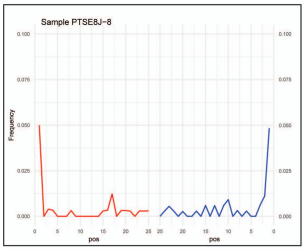

Fig. 5C: Sample PTSE8J-8, 1900 Q37 mapped reads.

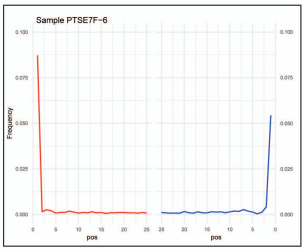

Fig. 5F: Sample PTSE7F-6, 221248 Q37 mapped reads.

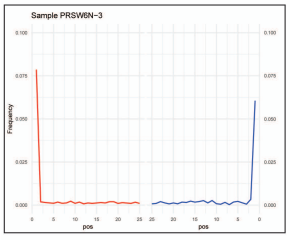

Fig. 5I: Sample PRSW6N-3, 73800 Q37 mapped reads.

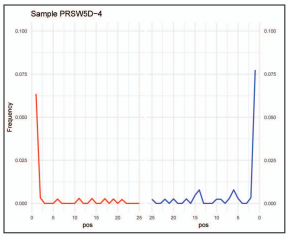

Fig. 5L: Sample PRSW5D-4, 2227 Q37 mapped reads.

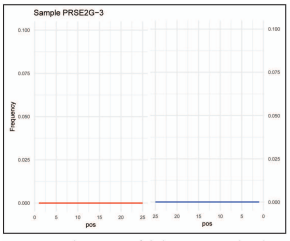

Fig. 5M: Sample PRSE2G-3, failed, 1 Q37 mapped reads.

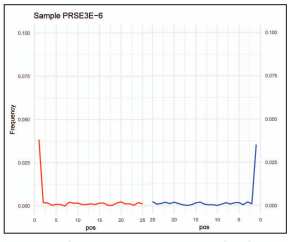

Fig. 5P: Sample PRSE3E-6, 23561 Q37 mapped reads.

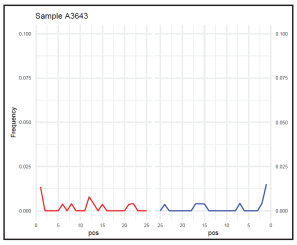

Fig. 5S: Sample A3643, 94078 Q37 mapped reads.

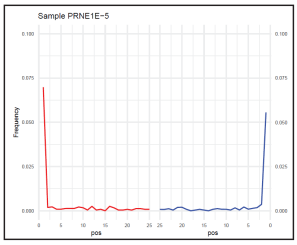

Fig. 5V: Sample PRNE1E-5, 24083 Q37 mapped reads.

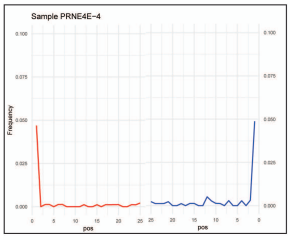

Fig. 5N: Sample PRNE4E-4, 5440 Q37 mapped reads.

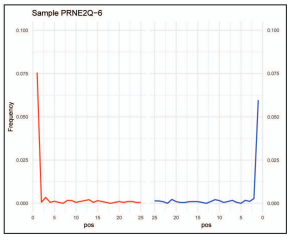

Fig. 5Q: Sample PRNE2Q-6, 18168 Q37 mapped reads.

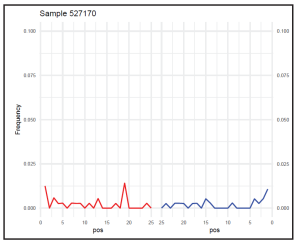

Fig. 5T: Sample 527170, 3177 Q37 mapped reads.

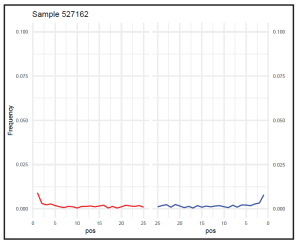

Fig. 5W: Sample 527162, 82559 Q37 mapped reads.

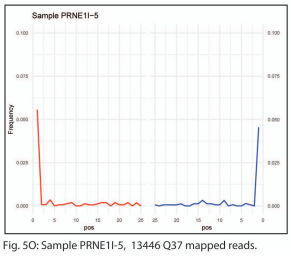

Fig. 5O: Sample PRNE1I-5, 13446 Q37 mapped reads.

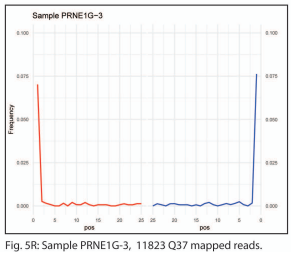

Fig. 5R: Sample PRNE1G-3, 11823 Q37 mapped reads.

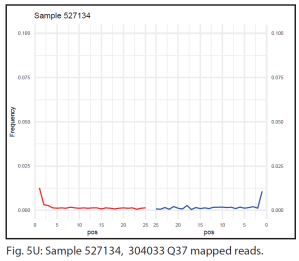

Fig. 5U: Sample 527134, 304033 Q37 mapped reads.

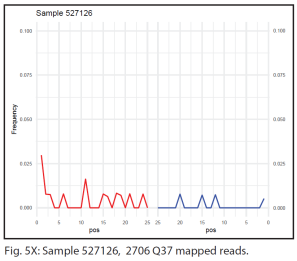

Fig. 5X: Sample 527126, 2706 Q37 mapped reads.

Fig. S5. Damage plots for all archaeological dentine and historical calculus mitogenomes.

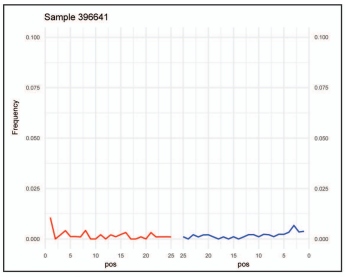

Fig. 5Y: Sample 396641, 12527 Q37 mapped reads.

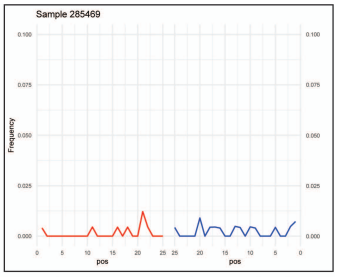

Fig. 5BB: Sample 285469, 26969 Q37 mapped reads.

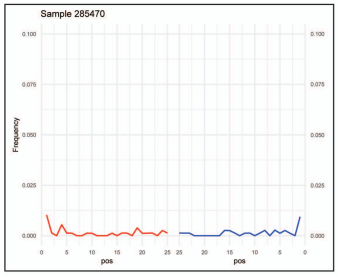

Fig. 5Z: Sample 285470, 56307 Q37 mapped reads.

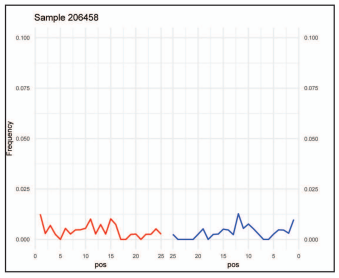

Fig. 5CC: Sample 206458, 5728 Q37 mapped reads.

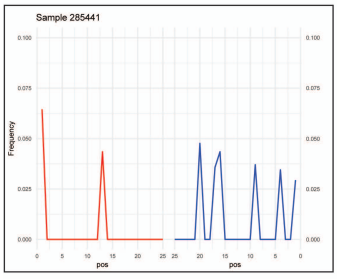

Fig. 5AA: Sample 285441, 2229 Q37 mapped reads.

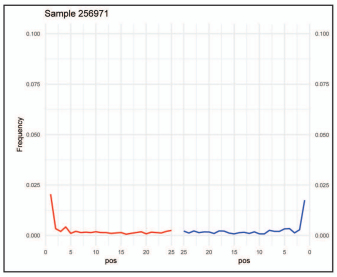

Fig. 5DD: Sample 256971, 78499 Q37 mapped reads.

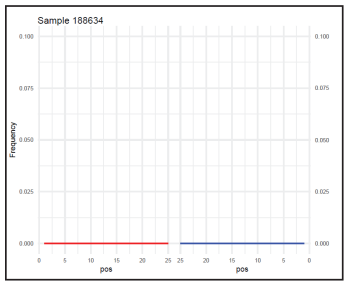

Fig. 5EE: Sample 188634, failed, 17 Q37 mapped reads.

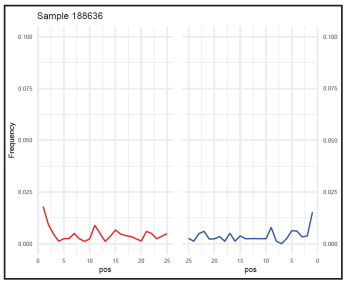

Fig. 5GG: Sample 188636, 7386 Q37 mapped reads.

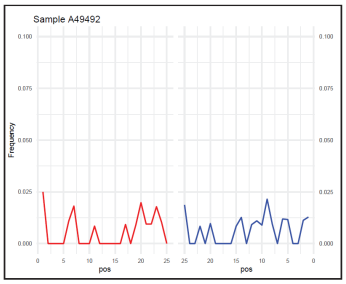

Fig. 5FF: Sample A49492, 4056 Q37 mapped reads.

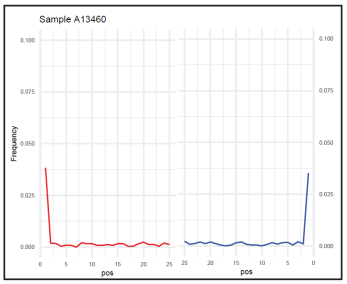

Fig. 5HH: Sample A13460, 7386 Q37 mapped reads.

Fig. S5. Damage plots for all archaeological dentine and historical calculus mitogenomes.

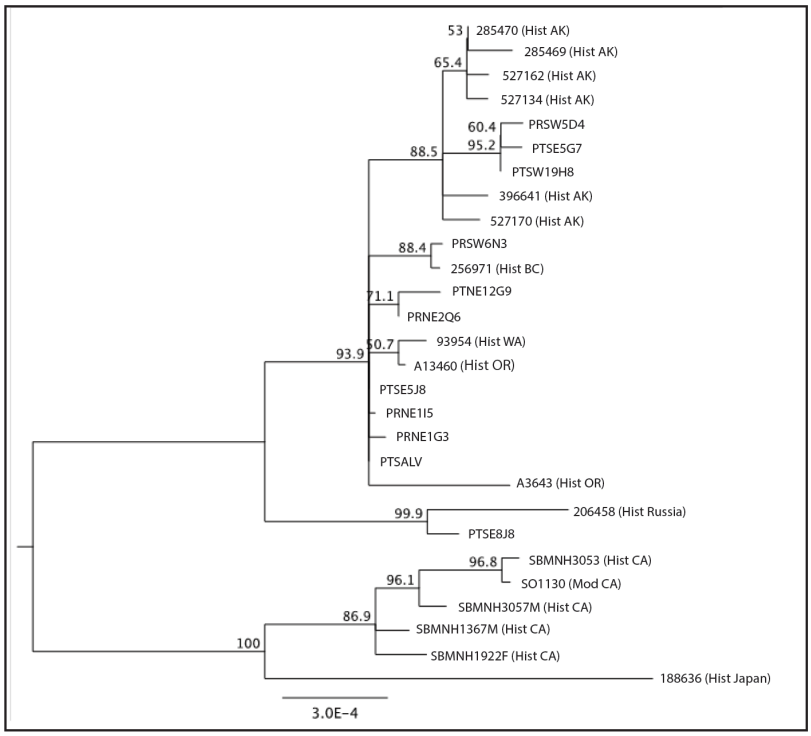

Fig. S6. Neighbor-joining phylogeny of representative ancient and modern sea otter mito-mitogenomes. Phylogeny built with Geneious Tree Builder and 1000 bootstrap replicates using Jukes-Cantor model. Bootstrap values are displayed on the nodes and scale indicates substitutions per site.

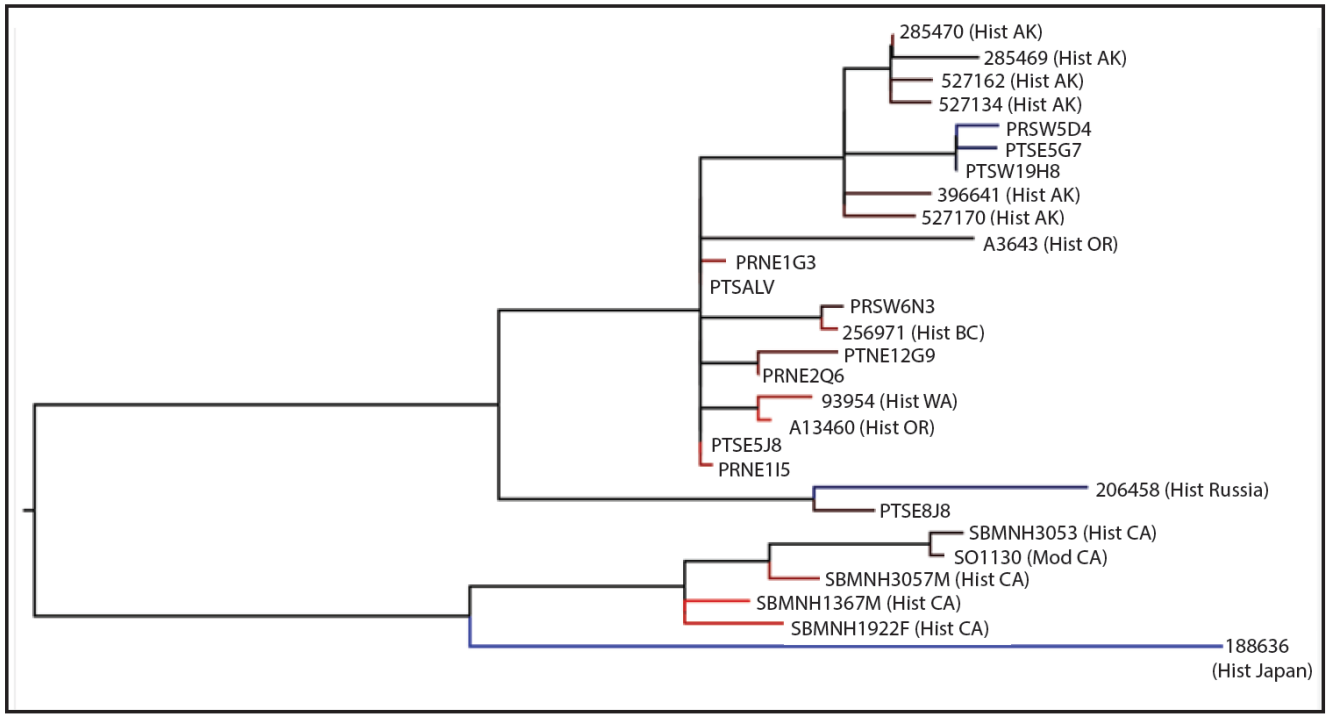

Fig. S7. TempEst analysis of neighbor joining phylogeny of sea otter mitogenomes. Samples with sequence divergence greater than expected given their age have red branches while those branches with less divergence than sampling age are blue.

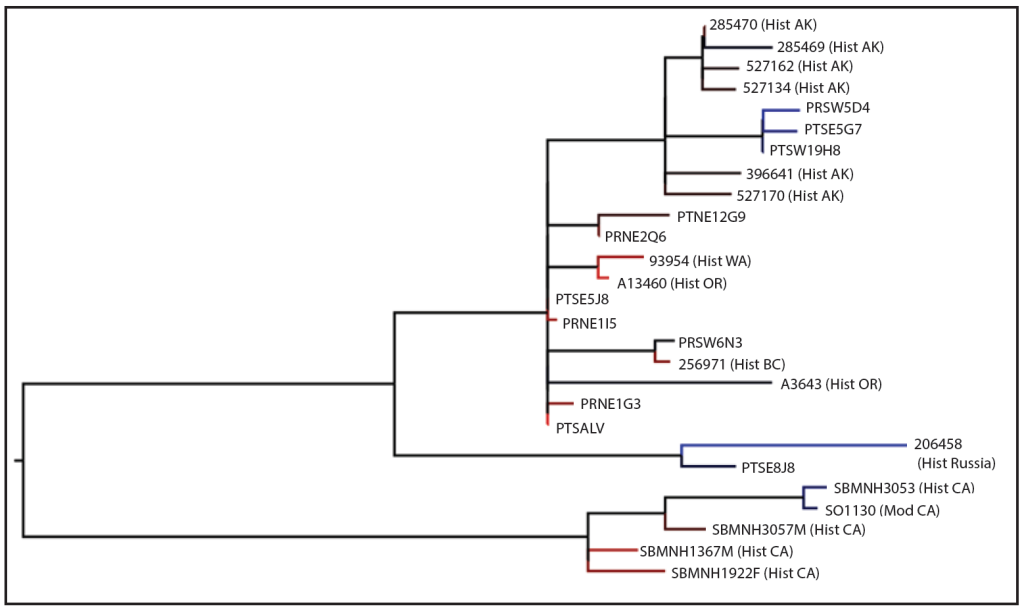

Fig. S8. TempEst analysis of neighbor joining phylogeny of sea otter mitogenomes without 188636. Samples with sequence divergence greater than expected given their age have red branches while those branches with less divergence than sampling age are blue.

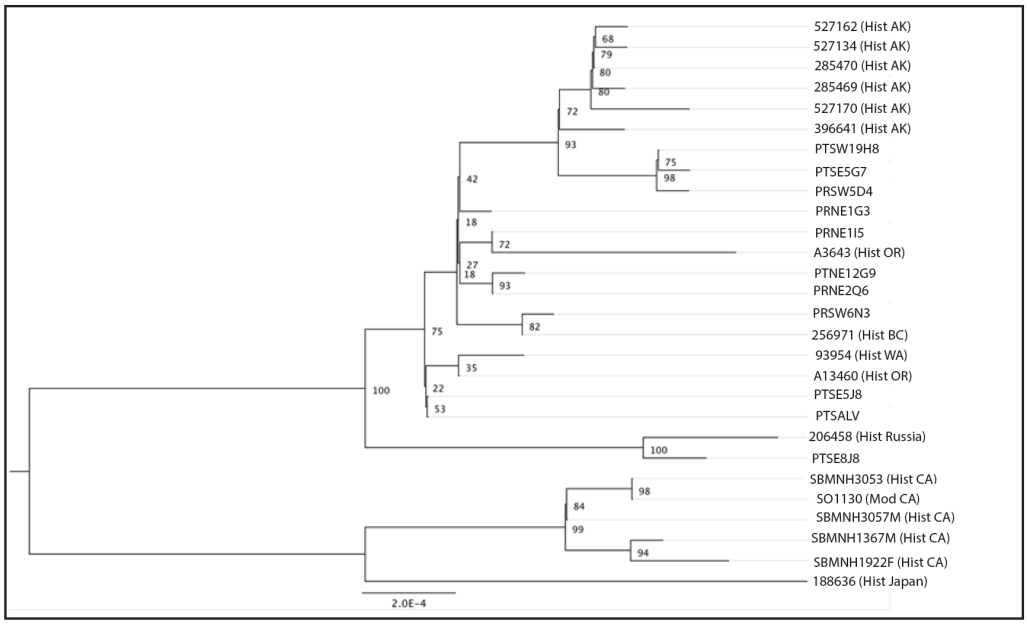

Fig. S9. Maximum likelihood phylogenetic analysis of sea otter mitogenomes built using IQ-TREE with 1000 bootstrap replicates. Bootstrap values are displayed on the nodes and scale indicates substitutions per site.

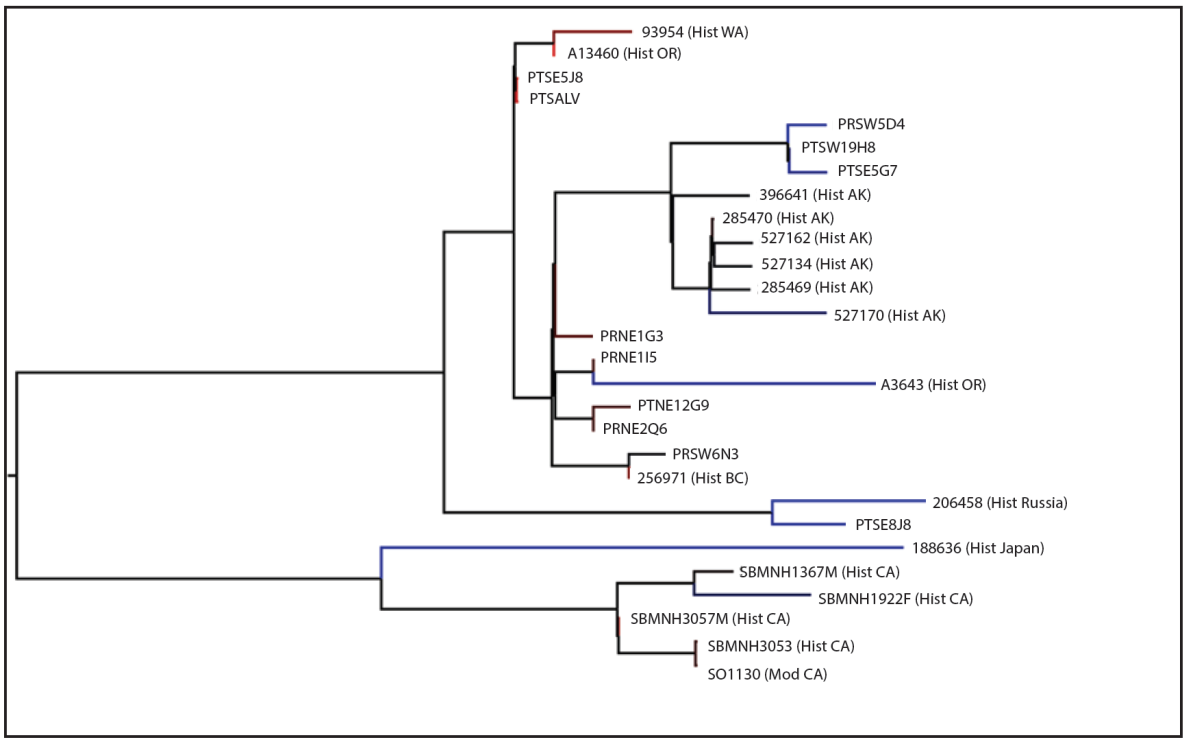

Fig. S10. TempEst analysis of maximum likelihood phylogeny of sea otter mitogenomes using IQ-TREE generated in Fig. S9. The phylogeny yields poor temporal results (R squared = 9.3485E-2).